Intelligent Service Robotics manuscript No.
(will be inserted by the editor)

Odest Chadwicke Jenkins

Sparse Control for High-DOF Assistive Robots

Received: date / Accepted: date

Abstract Human control of high degree-of-freedom robotic systems can often be difficult due to a **sparse control problem**. This problem relates to the disparity in the amount of information required by the robot's control variables and the relatively small volume of information a human can specify. To address the sparse control problem, we propose the use of subspaces embedded within the pose space of a robotic system. Driven by human motion, our approach is to uncover 2D subspaces using dimension reduction techniques that allow cursor control, or eventually decoding of neural activity, to drive a robotic hand. We investigate the use of five dimension reduction and manifold learning techniques to estimate a 2D subspace of hand poses for the purpose of generating motion. The use of shape descriptors for representing hand pose is additionally explored for dealing with occluded parts of the hand during data collection. We demonstrate the use of 2D subspaces of power and precision grasps for driving a physically simulated hand from 2D mouse input.

Keywords Assistive Robotics · Robot Manipulation · Manifold Learning · Motion Capture

This work was supported in part by ONR Award N000140710141, ONR DURIP "Instrumentation for Modeling Dexterous Manipulation", and NSF Award IIS-0534858.

Odest Chadwicke Jenkins
115 Waterman St.
Department of Computer Science
Brown University
Providence, RI 02912-1910
Tel.: +1-401-863-7600
Fax: +1-401-863-7657
E-mail: cjenkins@cs.brown.edu

1 Introduction

Developing human interfaces for controlling complex robotic systems, such as humanoid robots and mechanical prosthetic arms, presents an underdetermined problem. Specifically, the amount of information a human can reasonably specify within a sufficiently small update interval is often far less than a robot's degrees-of-freedom (DOFs). Consequently, basic control tasks for humans, such as reaching and grasping, are often onerous for human teleoperators of robot systems, requiring either a heavy cognitive burden or overly slow execution. Such teleoperation problems persist even for able-bodied human teleoperators given state-of-the-art sensing and actuation platforms.

The problem of teleoperation becomes magnified for applications to assistive robotics and, more generally, control of devices by users with physical disabilities. In such applications, feasible sensing technologies, such as electroencephalogram (EEG) [18], electromyography (EMG) [12,27,6,4], and cortical neural implants [8,22], provide a limited channel for user input due to the sparsity of information as well as the noise contained in the sensed signals. Specifically for **neural decoding**, efforts to produce control signals from neural activity have demonstrated success limited to 2-3 DOFs with bandwidth (estimated liberally) at around 10 bits/sec [19]

With such limited bandwidth, control applications have focused on low-DOF systems, such as 2D cursor control [21], planar mobile robots [18], 4 DOF finger motion [1], and discrete control of 4 DOF robot arms [11,6]. In scaling to higher-DOF systems, previous work could roughly be cast into two categories, **shared control** and **supervised action selection** from neural decoding. As described by Kim et al. [14], shared control can be seen as a behavior-based system [2] where the human provides high-level control and supervision that is refined and executed by autonomous low-level motion control procedures. Alternatively, current action (or pose) selection techniques divide the space of user input for supervision into discrete decision regions, each mapped to a particular robot action or pose. Bitzer and van der Smagt [4], using kernel-based classification techniques, have interactively controlled a high-DOF robot hand by classifying EMG data into a discrete set of poses. Work by Hochberg et al. [11] takes a similar approach by associating manually-chosen regions on a screen with robot actions (e.g., grasp object) for cursor-driven robot control of a 4 DOF robot arm and gripper. It is clear that such manually-crafted mappings between user input and robot pose spaces is a viable approach to supervised action selection. However, such mappings do not necessarily allow for scaling towards a wide variety of robot behavior. For example, the majority of existing work focuses on specific types power grasps for objects, which is a small fraction of the Cutkoski grasp taxonomy [7]. If users wish to perform more dexterous manipulation of objects, such as precision grasping of a fork or pencil, it is uncertain how they would select such actions for a control mapping suited to power grasping.

The question we pose is how to scale supervised action selection mappings to increasingly diverse types of behavior, which we address through "unsu-

pervised" dimension reduction techniques[1]. Robotic systems geared for general functionality or a human anthropomorphism will have significantly more than 2-3 DOFs, posing a **sparse control** problem. For instance, a prosthetic arm and hand could have around 30 DOF. While this mismatch in input and control dimensionality is problematic, it is clear that the space of valid human arm/hand poses does not fully span the space of DOFs. It is likely that plausible hand configurations exist in a significantly lower dimensional subspace arising from biomechanical redundancy and statistical studies of human movement [15, 24, 16, 5]. In general, the uncovering intrinsic dimensionality of this subspace is crucial for bridging the divide between decoded user input and the production of robot control commands.

In addressing the sparse control problem, our objective is to discover 2D subspaces of hand poses suitable for interactive control of a high-DOF robot hand, with the longer-term goal sparse control with 2D cursor-based neural decoding systems. We posit viable sparse control subspaces should be **scalable** (not specific to certain types of motion), **consistent** (two dissimilar poses are not proximal/close in the subspace), and **continuity-preserving** (poses near in sequence should remain proximal in the subspace). To uncover control subspaces, we follow a **data-driven** approach to this problem through the application of manifold learning (i.e., dimension reduction) to hand motion data, and motion captured from real human subjects.

In this short paper, we investigate the use of various dimension reduction techniques to estimate a 2D subspace of hand poses for the purpose of sparse human control of robot hands. Our aim is to uncover a 2D parameterization that transforms sparse user input trajectories into desired hand movements. Our current work focuses on *data-driven* methods for analyzing power and precision grasps obtained through optical motion capture. In our initial and ongoing experimentaion, we apply five dimension reduction techniques for embedding this data in a 2D coordinate space: Principal Components Analysis (PCA) [10], Hessian LLE [9], Isomap [23], Windowed Isomap, and Spatio-temporal Isomap [13]. The use of shape descriptors for representing hand pose is additionally explored for dealing with occluded parts of the hand during data collection. We demonstrate the use of uncovered 2D hand pose parameterizations of power and precision grasps to drive a physically simulated hand and 13 DOF robot hand from 2D mouse input.

2 The Sparse Control Problem

Our objective is to estimate a sparse control mapping $s : Z \rightarrow X$ that maps 2-dimensional user input $z \in \Re^d$ ($d = 2$) into the space of hand poses $x \in \Re^D$. d and D are the number of DOFs expressing human user input and robot hand pose, respectively. Shown in Figure (1), sparse control mapping sits within a feedback control loop of a human-robot team, serving as a control intermediary between a human decision maker and a robot platform. In this scenario, we assume an environment described at time t with state x_t whose

[1] "Unsupervised" in the context of machine learning refers to estimating the outputs of an unknown function given only its inputs.

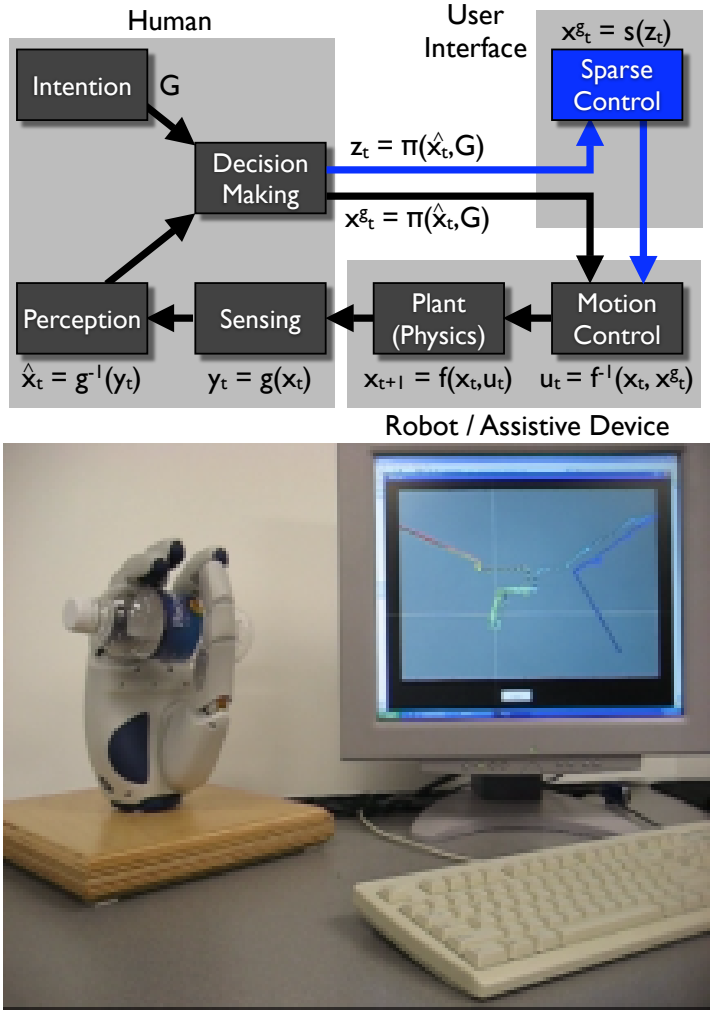

Fig. 1 (left) A diagram of the feedback control consisting of a human decision maker percieving robot state and generating action selection commands. Highlighted in blue, sparse control addresses the situation when the human has limited (sparse) communications with the robot, significantly less than robot's DOFs. (right) Snapshot of a sparse control system, from work by Tsoli and Jenkins [25], with the DLR robot hand driven by a human to grasp a water bottle.

physical integration is described by a (not necessarily known) function f. The robot is also assumed to have a motion control routine that produces appropriate motor commands given a desired state x_t^g (or goal robot pose) from a decision making routine. The human in the loop is responsible for making decisions to produce x_t^g, based on an internal policy π and intentions G, from their perception of state $\hat{x}_t$ from partial observations y. The user

interface is the medium through which the human user specifies the desired pose x_t^g to the robot platform.

The problem addressed in sparse control pertains to when the human cannot or is overly burdened in specifying the desired pose x_t^g for the robot. Specifically, we assume number of variables $D >> d*$, where $x_t^g \in \Re^D$, $z_t^* \in \Re^d*$, and z_t^* is the optimal amount of information a given that human can communicate to a robot. Obviously, z_t^* is a moving limit that varies for each individual human user. However, given most people can function with a 2D mouse input device, we assume $d^* << 2$ and seek to find a functional mapping $x_t^g = s(z_t)$ where $z_t \in \Re^2$. Further, efforts in neural decoding [11, 22, 20] have shown that disabled individuals physically incapable of moving 2D mouse can drive a 2D cursor from neural activity.

Our estimation of the mapping s is founded upon the assumption that the space of plausible hand poses is intrinsically parameterized by a low-dimensional manifold subspace. We assume each hand pose achieved by a human is an example generated within this manifold subspace. It is given that the true manifold subspace of hand poses is likely to have dimensionality greater than two. With an appropriate dimension reduction technique, however, we can preserve as much of the intrinsic variance as possible. As improvements in decoding occur, the dimensionality and fidelity of the input signal will increase but the same control mapping infrastructure can leveraged without modification.

We create a control mapping by taking as input a set of observed training hand poses $z_i \in \Re^D$, embedding this data into latent user control space coordinates $z_i \in \Re^2$, and generalizing to new poses through out-of-sample projections. Although 2D locations can be manually assigned to hand poses, as an approximation to the latent inverse mapping $z_i = s^{-1}(x_i)$, we assume such procedures will lack scalability as new functionality becomes desired. In contrast, we take a data-driven approach using dimension reduction, namely manifold learning tecniques. Dimension reduction estimates the latent coordinates z such that distances between datapairs preserve some criteria of similarity. Each dimension reduction method has a different notion of pairwise similarity and, thus, a unique view of the intrinsic structure of the data. Once embedded, the input-control pairs (x_i, z_i) are generalized through interpolation to allow for new (out-of-sample) points [3] to be mapped between user input and pose spaces.

2.1 Dimension Reduction Overview

Our method relies upon a suitable notion of pairwise similarity for performing dimension reduction. We explored the use of five dimension reduction methods for constructing control mappings: Principal Components Analysis (PCA) [10], geodesic Multidimensional Scaling (Isomap) [23], Hessian LLE (HLLE) [9], temporally-windowed Isomap (Windowed Isomap), and Spatio-temporal Isomap (ST-Isomap) [13]. The first method, PCA, constructs a linear transform of rank 2 A about the mean of the data μ:

$$z = s^{-1}(x) = A(x - \mu) \tag{1}$$

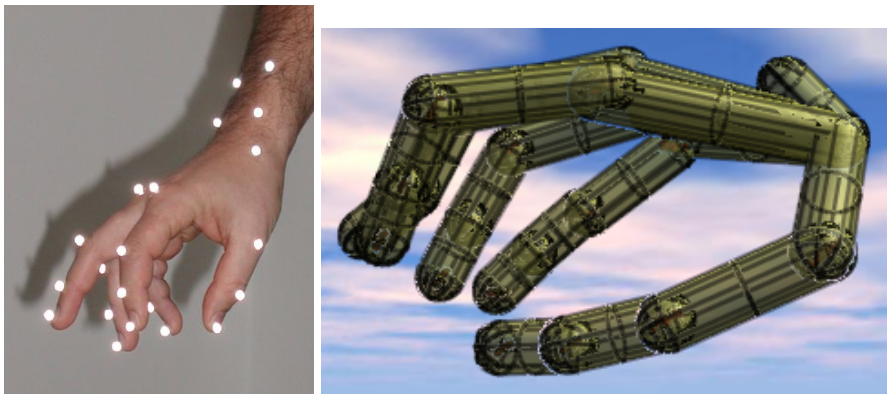

Fig. 2 (top) Snapshot of a hand instrumented with reflective markers for optical motion capture. (bottom) Our physically simulated hand attempting to achieve the captured hand configuration above.

PCA is equivalent to performing multidimensional scaling (MDS) [10] with pairwise Euclidean distance. MDS is a procedure that takes a full matrix M, where each element $M_{x,x'}$ specifies the distance between a datapair, and produces an embedding that attempts to preserve distances between all pairs. MDS is an optimization that minimizes the "stress" E of the pairwise distances:

$$E = \sqrt{\sum_{x} \sum_{x'} (\sqrt{(f(x) - f(x'))^2}) - M_{x,x'})^2} \tag{2}$$

The second method, Isomap, is MDS where shortest-path distances are contained in M as an approximation of geodesic distance:

$$M_{x,x'} = \min_p \sum_i M'(p_i, p_{i+1}) \tag{3}$$

where M' is a sparse graph of local distances between nearest neighbors and p is a sequence of points through M' indicating the shortest path. Isomap performs nonlinear dimension reduction by transforming the data such that geodesic distance along the underlying manifold becomes Euclidean distance in the embedding. A canonical example of this transformation is the "Swiss roll" example, where input data generated by 2D manifold is contorted into a roll in 3D. Given a sufficient density of samples, Isomap is able to flatten this Swiss roll data into its original 2D structure, within an affine transformation.

PCA and Isomap assume input data are unordered (independent identical) samples from the underlying manifold, ignoring the temporal dependencies between successive data points. However, human hand motion has a sequential order due to the temporal nature of acting in the real world. Windowed Isomap accounts for these temporal dependencies in a straightforward manner by windowing the input data $\tilde{x}_i = x_i \dots x_{i+w}$ over a horizon of length w. This augmentation of the input data effectively computes local distances

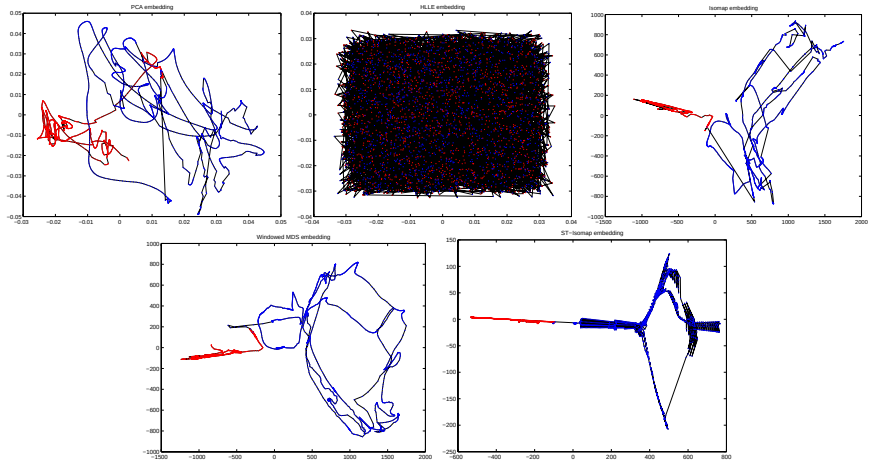

Fig. 3 Embedding of the hand marker positions using (in order) PCA , Hessian LLE, Isomap, windowed Isomap, and ST-Isomap. Power and precision grasp configurations are shown in blue and red, respectively. A black line is drawn between temporally adjacent configurations.

M' between trajectories from each input point rather than individual data points.

ST-Isomap further augments the local distances between the nearest neighbors of windowed Isomap. ST-Isomap reduces the distance between the local neighbors that are spatio-temporal correspondences, i.e., representative of the k best matching trajectories, to each data point. Distances between a point and its spatio-temporal correspondences are reduced by some factor and propagated into global correspondences by the shortest-path computation. The resulting embedding attempts to register these correspondences into proximity. In this respect, ST-Isomap is related to time-sereies registration using Dynamic Time Warping [17]. The distinctions are that ST-Isomap does not require segmented or labeled time-series and uses a shortest-path algorithm for dynamic programming.

All of these methods assume the structure of the manifold subspace is convex. Hessian LLE [9] avoids this convexity limitation by preserving local shape. Local shape about every data point is defined by an estimate of the Hessian $H_{x,x'}$ tangent to every point. $H_{x,x'}$ specifies the similarity of x to neighboring points x'; non-neighboring points have no explicit relationship to x. This sparse similarity matrix $\tilde{H}_{x,x'}$ is embedded in a manner similar to MDS, where global pairwise similarity is implicit in the local neighborhood connectivity.

3 Initial Results

The dimension reduction methods mentioned above were applied to human hand movement collected through optical motion capture. The performer's

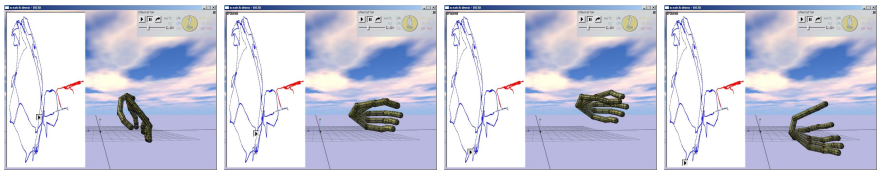

Fig. 4 A visualization controlling a power grasp for a physically simulated hand using 2D mouse control. A mouse trajectory in the windowed Isomap embedding (shown by the cursor position) is mapped into hand configurations. This trajectory shows an initial idle configuration, preshaping, grasp closure, and rotation.

hand was instrumented with 25 reflective markers, approximately .5cm in width, as shown in Figure 2. These markers were placed at critical locations on the top of the hand: 4 markers for each digit, 2 for the base of the hand, and 3 on the forearm. A Vicon motion capture system localized each of these markers over time.

The human performer executed several power and precision grips with different orientations of the hands. Power grasps involved the human closing all their fingers and thumb around a hypothetical cylindrical object with a diameter of 1.5in. Precision grasps consisted of the thumb making contact with each finger individually. The resulting dataset consisted of approximately 3000 frames of 75 DOF data (25 markers in 3D). Markers that dropout (occluded such that their location cannot be estimated) were assigned a default location during intervals of occlusion.

Embeddings produced by each of the dimension reduction methods are shown in Figure 3, with neighborhoods $k = 5$ for HLLE, $k = 50$ (Isomap), $k = 10$ (windowed Isomap), $k = 3$ (ST-Isomap). Windowing occurred over a 10 frame horizon. ST-Isomap reduced distances by a factor of 10 between points that are the $k = 3$ best local correspondences.

The quality of each embedding was assessed based on the properties of *consistency*, embedding locations that merge disparate hand configurations, and *temporal continuity*, preserving the proximity of poses that are sequentially adjacent. Inconsistency is an undesired artifact that is related to residual variance (or stress) not accounted for in the embedding. The effect of residual variance differs across methods and is only of consequence with respect to inconsistency. We were unable to find a reasonable embedding for HLLE, suggesting the space of marker configurations does have continuous local shape. The PCA embedding best preserves the consistency among the precision grasps. However, this embedding has many temporal discontinuities due to marker dropout and inconsistencies for power grasps. The Isomap embedding suffers from the same discontinuities with fewer inconsistencies of the power grasp and greater inconsistencies of the precision grasp. The windowed Isomap embedding removes the discontinuities of the Isomap embedding by effectively performing a square wave low-pass filter on the input before shortest-path computation. The ST-Isomap embedding was prone to overregistration of the data, which we attribute to a lack of adaptivity in the number of correspondences across local neighborhoods.

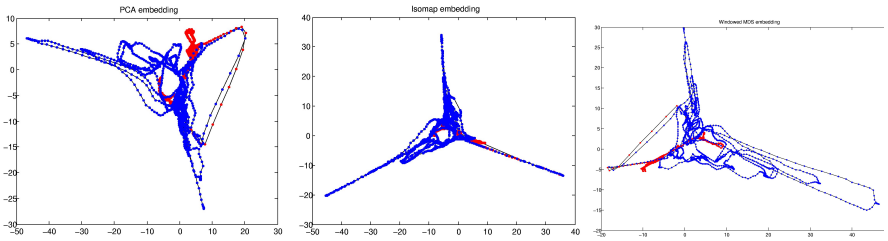

Fig. 5 Embedding of the centralized moments for hand marker positions using (left-to-right) PCA, Isomap, and windowed Isomap. Power and precision grasp configurations are shown in blue and red, respectively. A black line is drawn between temporally adjacent configurations.

The quality of each embedding with respect to sparse robot control was performed by driving a physically simulated robot hand. The simulated hand consisted of 27 DOFs: 4 DOFs per finger, 7 thumb DOFs, and 6 wrist DOFs for position and orientation global coordinates. The kinematics of the hand were created manually using the marker positions from a single frame in the data set. Cylindrical geometries were used to represent the hand. Our simulation engine, described in [26], used the Open Dynamics Engine to integrate physics over time. The desired configuration of the hand is set by the nearest neighbor in the 2D embedding of the current mouse position. Motion control of the hand was performed using our implementation of Zordan and van der Horst's optical motion capture control procedure [28]. This motion controller takes a desired pose as the 3D locations of a set of uniquely identified markers that have corresponding locations on the hand. Springs of critical damping are attached between each desired marker location and corresponding location on the hand. The equilibrium of these springs brings the hand to rest at the desired hand pose.

Shown in Figure 4, a human user is able to move a cursor around the embedding to perform simple power grasping with the Windowed Isomap embedding. Although we found the windowed Isomap embedding to be the most promising, none of these methods appeared to be directly applicable to yield reasonable input spaces for sparse control. The problem namely stems from how precision grasps are embedded into 2D. Our intuition is that proper estimation of nearest neighbors is difficult to achieve. As a result, "short circuits" are created in the shortest path and cause inconsistency in the embedding. Consequently, control over precision grasps often causes the system to be unstable due to violent changes in the hand pose desireds from a small mouse movement in certain areas of the embedding. As future work, we are exploring the use of graph denoising techniques, such as through belief propagation algorithms [25], to allow for embedding of a larger number of types of hand motion while preserving consistency and continuity.

Marker dropout from occluded parts of the hand was also a large factor in the embedding inconsistency and discontinuity. To account for marker dropout, statistical shape descriptors were used to recast the input space with features less sensitive to specific marker positions. Centralized moments [10] up through the 16th order were computed for the non-occluded markers at

every frame of the motion. The resulting data set contained 3000 data points with 4096 dimensions and was used as input into PCA, Isomap (k=20), and windowed Isomap (k=5). As shown in Figure 5, all three of these methods produced embeddings with three articulations from a central concentrated mass of poses, have better consistency between power and precision grasps, and exhibit no significant discontinuities. From our preliminary control tasks, the PCA embedding provides the best spread across the 2D space with comparable levels of consistency to windowed Isomap.

4 Conclusion

We have presented the sparse control problem in human control of high-DOF robotic and assistive devices. Viewing the human-robot collaboration, we consider the case where a human user cannot specify, through a user interface, the number of variables needed to express a desired robot pose. We have explored the use of dimension reduction for estimating low-dimenional 2D subspaces in such controlling high DOF control scenarios. Our aim in this work has been to provide a means for controlling high dimensional systems with sparse 2D input by leveraging current decoding capabilities. We have taken a data-driven approach to this problem by using dimension reduction to embed motion performed by humans into 2D. Five dimension reduction methods were applied to motion capture data of human performed power and precision grasps. Centralized moments were utilized towards embedding with greater consistency and utilization of the embedding space. Using our embeddings, successful control of power grasps was achieved, but execution of precision grasping and other forms of hand movement require further study. We estimate that greater exploration of neighborhood graph denoising and shape descriptors suitable for embedding hand poses offers an avenue for addressing these issues for functional sparse control for object manipulation.

Acknowledgements The author thanks Aggeliki Tsoli, Morgan McGuire, Michael Black, Greg Shaknarovich, and Mijail Serruya for simulation, motion data assistance, and helpful discussions.

References

1. Afshar, P., Matsuoka, Y.: Neural-based control of a robotic hand: Evidence for distinct muscle strategies. In: IEEE International Conference on Robotics and Automation) (2004)
2. Arkin, R.C.: Behavior-Based Robotics. MIT Press, Cambridge, Massachusetts, USA (1998)
3. Bengio, Y., Paiement, J.F., Vincent, P.: Out-of-sample extensions for lle, isomap, mds, eigenmaps, and spectral clustering. In: Advances in Neural Information Processing Systems 16 (NIPS 2003). Vancouver, British Columbia, Canada (2003)
4. Bitzer, S., van der Smagt, P.: Learning emg control of a robotic hand: towards active prostheses. In: IEEE International Conference on Robotics and Automation (2006)

5. Ciocarlie, M., Goldfeder, C., Allen, P.: Dimensionality reduction for hand-independent dexterous robotic grasping. In: IEEE International Conference on Intelligent Robots and Systems (2007)
6. Crawford, B., Miller, K., Shenoy, P., Rao, R.: Real-time classification of electromyographic signals for robotic control. In: National Conference on Artificial Intelligence (AAAI 2006) (2005)
7. Cutkosky, M.: On grasp choice, grasp models, and the design of hands for manufacturing tasks. IEEE Transactions on Robotics and Automation **5**(3), 269–279 (1989)
8. Donoghue, J., Nurmikko, A., Friehs, G., Black, M.: Development of neural motor prostheses for humans. Advances in Clinical Neurophysiology (Supplements to Clinical Neurophysiology) **57** (2004)
9. Donoho, D., Grimes, C.: Hessian eigenmaps: Locally linear embedding techniques for high-dimensional data. Proc. National Academy of Sciences **100**(10), 5591–5596 (2003)
10. Duda, R.O., Hart, P.E., Stork, D.G.: Pattern Classification (2nd Edition). Wiley-Interscience (2000)
11. Hochberg, L., Serruya, M., Friehs, G., Mukand, J., Saleh, M., Caplan, A., Branner, A., Chen, D., Penn, R., Donoghue, J.: Neuronal ensemble control of prosthetic devices by a human with tetraplegia. Nature **442**, 164–171 (2006)
12. Iberall, T., Sukhatme, G.S., Beattie, D., Bekey, G.A.: On the development of emg control for a prosthesis using a robotic hand. In: IEEE International Conference on Robotics and Automation, pp. 1753–1758. San Diego, CA (1994)
13. Jenkins, O.C., Matarić, M.J.: A spatio-temporal extension to Isomap nonlinear dimension reduction. In: The International Conference on Machine Learning (ICML 2004), pp. 441–448. Banff, Alberta, Canada (2004).
14. Kim, H., Biggs, S., Schloerb, D., Carmena, J., Lebedev, M., Nicolelis, M., Srinivasan, M.: Continuous shared control stabilizes reach and grasping with brain-machine interfaces. IEEE Transactions on Biomedical Engineering **53**(6), 1164–1173 (2006)
15. Lin, J., Wu, Y., Huang, T.: Modeling the constraints of human hand motion. In: IEEE Workshop on Human Motion (2000)
16. Mason, C.R., Gomez, J.E., Ebner, T.J.: Hand synergies during reach-to-grasp. The Journal of Neurophysiology **86**(6), 2896–2910 (2001)
17. Myers, C.S., Rabiner, L.R.: A comparative study of several dynamic time-warping algorithms for connected word recognition. The Bell System Technical Journal **60**(7), 1389–1409 (1981)
18. del R. Millan, J., Renkens, F., Mourino, J., Gerstner, W.: Brain-actuated interaction. Artif. Intell. **159**(1-2), 241–259 (2004). DOI http://dx.doi.org/10.1016/j.artint.2004.05.008
19. Santhanam, G., Ryu, S.I., Yu, B.M., Afshar, A., Shenoy, K.V.: A high-performance brain-computer interface. Nature **442**, 195–198 (2006)
20. Serruya, M., Caplan, A., Saleh, M., Morris, D., Donoghue, J.: The braingate pilot trial: Building and testing a novel direct neural output for patients with severe motor impairment. In: Soc. for Neurosci. Abstr. (2004)
21. Serruya, M.D., Hatsopoulos, N.G., Paninski, L., Fellows, M.R., Donoghue, J.P.: Brain-machine interface: Instant neural control of a movement signal. Nature **416**, 141–142 (2002)
22. Taylor, D., Tillery, S.H., Schwartz, A.: Information conveyed through brain control: Cursor versus robot. IEEE Trans. Neural Systems Rehab Eng. **11**(2), 195–199 (2003)
23. Tenenbaum, J.B., de Silva, V., Langford, J.C.: A global geometric framework for nonlinear dimensionality reduction. Science **290**(5500), 2319–2323 (2000)
24. Todorov, E., Ghahramani, Z.: Analysis of the synergies underlying complex hand manipulation. In: Intl. Conference of the IEEE Engineering in Medicine and Biology Society (2004)
25. Tsoli, A., Jenkins, O.C.: 2d subspaces for user-driven robot grasping. In: Robotics: Science and Systems - Robot Manipulation: Sensing and Adapting to the Real World (2007).

26. Wrotek, P., Jenkins, O., McGuire, M.: Dynamo: Dynamic data-driven character control with adjustable balance. In: ACM SIGGRAPH Video Game Symposium. Boston, MA, USA (2006).
27. Zecca, M., Micera, S., Carrozza, M.C., Dario, P.: Control of multifunctional prosthetic hands by processing the electromyographic signal. Critical Reviews in Biomedical Engineering **30**(4-6), 459–485 (2002)
28. Zordan, V.B., Horst, N.C.V.D.: Mapping optical motion capture data to skeletal motion using a physical model. In: SCA '03: Proceedings of the 2003 ACM SIGGRAPH/Eurographics symposium on Computer animation, pp. 245–250. Eurographics Association, Aire-la-Ville, Switzerland, Switzerland (2003)